Cell Signaling

International Edition: DOI: 10.1002/anie.201505991
German Edition: DOI: 10.1002/ange.201505991

Label-Free Imaging of Dynamic and Transient Calcium Signaling in Single Cells

*Jin Lu and Jinghong Li**

Abstract: *Cell signaling consists of diverse events that occur at various temporal and spatial scales, ranging from milliseconds to hours and from single biomolecules to cell populations. The pathway complexities require the development of new techniques that detect the overall signaling activities and are not limited to quantifying a single event. A plasmonic-based electrochemical impedance microscope (P-EIM) that can provide such data with excellent temporal and spatial resolution and does not require the addition of any labels for detection has now been developed. The highly dynamic and transient calcium signaling activities at the early stage of G-protein-coupled receptor (GPCR) stimulation were thus studied. It could be shown that a subpopulation of cells is more responsive towards agonist stimulation, and the heterogeneity of the local distributions and the transient activities of the ion channels during agonist-activated calcium flux in single HeLa cells were investigated.*

Calcium (Ca^{2+}) is an important intracellular signaling agent that can impact numerous cell functions, including cell metabolism, gene expression, protein synthesis and modification, secretion, and apoptosis.[1] All of these functions simply originate from the existence of a steep gradient of the Ca^{2+} concentration across the cell membrane and the modulation of the intracellular Ca^{2+} concentration.[2] Ca^{2+} signaling displays varying temporal and spatial patterns, such as the amplitude of the Ca^{2+} spikes, the frequency of the Ca^{2+} waves, and the microdomains of the Ca^{2+} flickers.[3] Over the past decades, various synthetic or genetically encoded fluorescent calcium indicators have been developed to measure changes in the Ca^{2+} concentration in the cytosol, endoplasmic reticulum, and other organelles.[4] Fluorescence labeling enables one to focus on one specific signaling molecule and analyze Ca^{2+}-sensitive processes and Ca^{2+} signaling networks in detail. However, most cell signal transductions have complex pathway networks. Various proteins, receptors, and small molecules in different parts of the cell communicate with each other to regulate certain cellular functions. Therefore, multiple targets need to be manipulated by the label or over-expression, and large amounts of data need to be collected to study cell-signaling processes.

Alternatively, cell-signaling activities can be quantitatively evaluated by detecting the integrated cell response, which is often achieved with label-free spectroscopic or impedance techniques.[5] This pathway-unbiased signal simplifies the measurement of the complex signaling activities. Furthermore, this label-free strategy is sensitive enough to detect the cellular response of endogenous receptors. The intact cells can be assessed in a physiologically relevant environment, while avoiding any possible structure alterations or functional changes of the target molecule that could be induced during in situ labeling or over-expression in live cells.[6]

By combining a high-resolution, objective-based surface plasmon resonance microscope with AC potential modulation (AC = alternating current),[7] we developed a plasmonic-based electrochemical impedance microscope (P-EIM) that can provide valuable information without a requiring a label (Figure 1 a). The P-EIM can simultaneously record SPR (surface plasmon resonance) and EIM (electrochemical impedance microscopy) images of cells, aside from conventional transmission microscopy images (Figure 1 b). Herein, we used the P-EIM to study intracellular calcium signaling during the early stage of the histamine-triggered activation of G-protein-coupled receptors (GPCRs) in HeLa cells. GPCRs play a central role in regulating the intracellular Ca^{2+} concentration. For instance, extracellular hormones, neurotransmitters, or other stimuli can bind to cell-surface GPCRs (primarily of the Gq subtype), trigger an increase in the

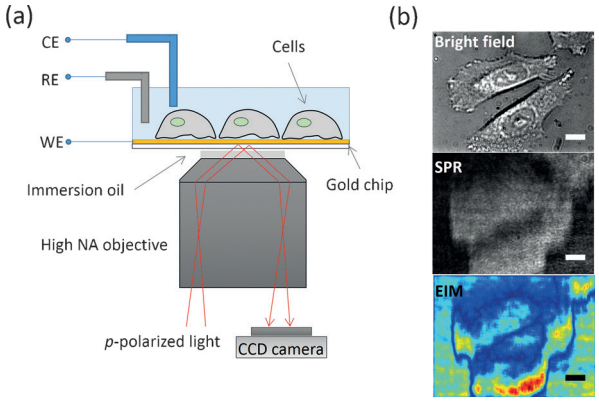

Figure 1. a) Setup of the plasmonic-based electrochemical impedance microscope (P-EIM). CE = counter electrode, NA = numeric aperture, RE = reference electrode, WE = working electrode. b) Bright-field, SPR, and EIM images of HeLa cells. Scale bar: 10 μm.

[*] Dr. J. Lu, Prof. Dr. J. Li
Department of Chemistry, Beijing Key Laboratory for Microanalytical Methods and Instrumentation, Tsinghua University
Beijing 100084 (China)
E-mail: jhli@mail.tsinghua.edu.cn

Supporting information for this article is available on the WWW under http://dx.doi.org/10.1002/anie.201505991.

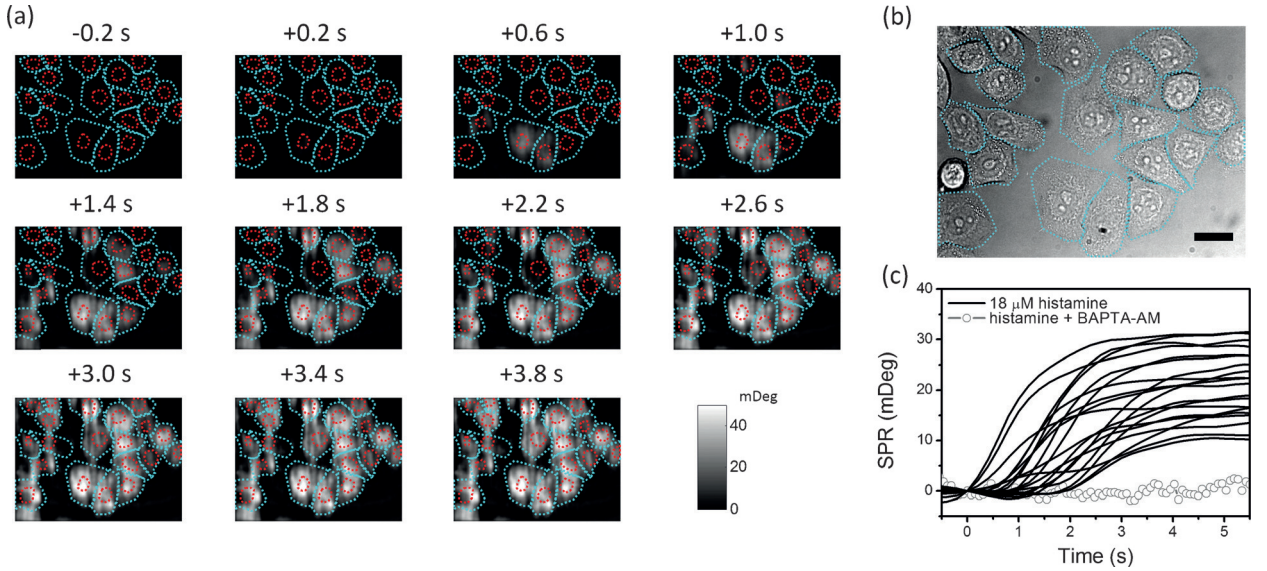

Figure 2. a) Differential SPR images recorded at 0.4 s intervals during the first 3.8 s after treatment with 18 μM histamine. The cyan and red dotted lines represent the boundaries of individual cells and the nuclei, respectively, and were obtained from the transmission images in (b). Scale bar: 20 μm. c) SPR response curves (black lines) of individual cells stimulated by histamine, and average SPR response of multiple cells to histamine stimulation after pretreatment with 10 μM BAPTA-AM for 20 min (gray circles).

intracellular Ca^{2+} concentration, and activate various Ca^{2+}-sensitive processes to control a wide variety of metabolic and differentiated functions.[8]

Benefiting from the high tempo-spatial resolution of P-EIM imaging, we were able to record raw P-EIM images every 7 ms (137 fps) and obtained both SPR and EIM images with the individual cells clearly resolved. In the first few seconds after histamine stimulation, an obvious increase of the SPR signals from the HeLa cells was observed (Figure 2a). During this short period, several cellular events were activated, including histamine binding to the H1 receptor, elevation of the cytosolic inositol trisphosphate (IP_3) concentration, and Ca^{2+} release from the endoplasmic reticulum (ER).[1b,9] Although these events cannot be directly detected by SPR (see the Supporting Information, Section S2), we believe that the increase in the SPR signal is related to the calcium flux activity. First, fluorescence images of intracellular calcium show that the intracellular Ca^{2+} concentration undergoes a rapid increase within seconds after histamine treatment, and the time scale is in good agreement with the SPR observation (Section S3).[9c] Next, we pretreated the HeLa cells with BAPTA-AM [1,2-bis(2-aminophenoxy)-ethane-*N*,*N*,*N*′,*N*′-tetraacetic acid tetrakis(acetoxymethyl ester)], which can penetrate the cell membrane and chelate intracellular calcium. In this case, no SPR response was observed after histamine activation (gray circles in Figure 2c and SPR images in Figure 5b). During IP_3 mediated Ca^{2+} release, the ER plays an important role as a prime intracellular Ca^{2+} store. The depletion of Ca^{2+} in the ER affects its morphology, function, and communication with other organelles.[10] In particular, micromotions of the ER lead to changes in the local refractive index or the cellular mass redistribution, which can be detected by SPR. The ER is known as a highly dynamic, interconnected reticular network of tubules around the nuclear region, which is in good agreement with the observation that the SPR response mainly came from the center of the cell (Figure 2a and Movie S1).

In-depth kinetic analyses of the single-cell SPR response further describe how the calcium flux activities vary in individual cells. The time-sequence SPR images and response curves (Figure 2) show that each cell profile had its own characteristic onset time (t_0), which was followed by an initial exponential increase (with rate constant k) of the SPR signal, and then reached a plateau (SPR_{max}). The SPR responses of 59 cells are summarized in the scatter diagram in Figure 3. It clearly shows that cells with shorter latency always display a stronger and faster SPR response (red/orange dots in the upper right corner of Figure 3), indicating that a subpopula-

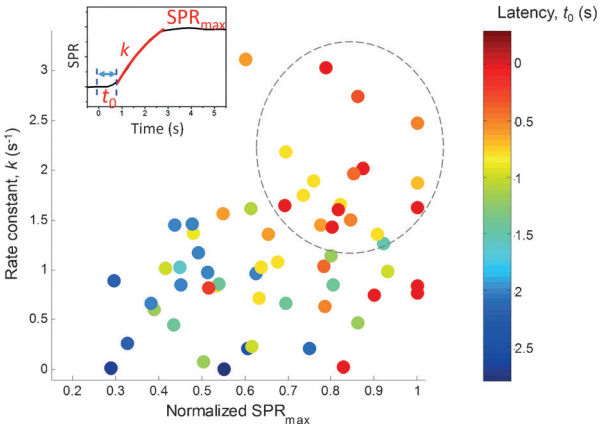

Figure 3. Scatter diagram of the rate constant (k) and the normalized SPR_{max} response of 59 cells. The color of the dots represents the onset time (latency, t_0). Inset: diagram to illustrate the definitions of t_0, k, and SPR_{max} for a single-cell SPR response curve. k is the rate constant obtained by fitting of the initial ramp of the SPR curve to $SPR(t) = a(1-e^{-kt}) + c$ (Section S4).

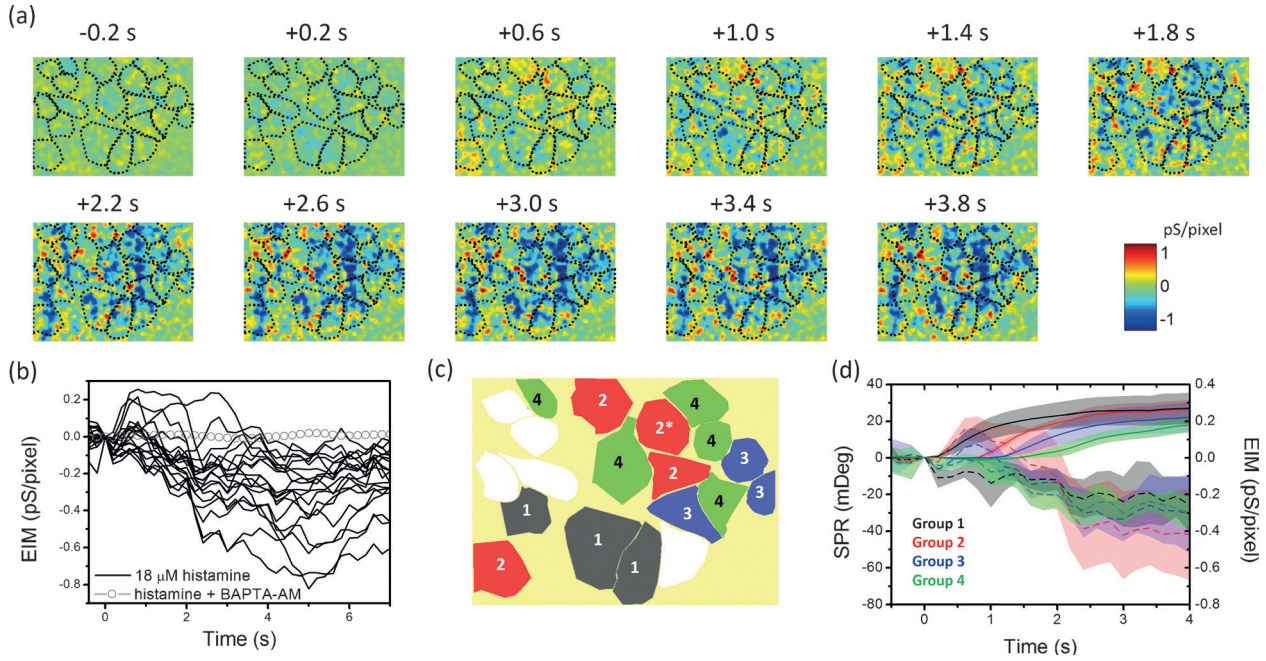

Figure 4. a) Differential EIM images recorded at 0.4 s intervals during the first 3.8 s after treatment with 18 μM histamine. The black dotted lines represent the boundaries of individual cells and were obtained from the transmission images. b) EIM response curves (black lines) of individual cells stimulated by histamine, and average EIM response of multiple cells to histamine stimulation after pretreatment with 10 μM BAPTA-AM for 20 min (gray circles). c) The cells were classified into four groups according to their average SPR latencies: 0 s (gray, group 1), 0.8 s (red, group 2), 1.2 s (blue, group 3), and 1.6 s (green, group 4) . d) Average SPR (solid) and EIM (dashed) response curves of cells of a particular group. The shaded regions represent the standard deviation of the single-cell response for each group.

tion of the cells is more active towards agonist stimulation. These variations could be attributed to differences in the expression levels of the Ca^{2+} signaling receptors, the probabilities of the IP_3 channels being open, the capacities of the ER for internal Ca^{2+} storage, and the cell cycle status,[11] which result in strikingly different response kinetics.

Simultaneously, single-cell EIM information can also be extracted from the raw P-EIM images (Figure 4a). Unlike SPR, EIM detects changes in the local dielectric and conductive properties.[7c,d] During agonist-induced calcium flux, the micromotions of the ER increase the local refractive index as the cellular structure changes, which in turn gives rises to stronger SPR signals and weaker EIM signals (Figure 4b).

To further study the single-cell EIM response, cells were selected and classified into four groups based on their SPR latency (Figure 4c,d, see also Section S5). A transient (1–2 s) positive EIM response was observed for cells in groups 2 and 3 (Figure 4d), before the EIM signals became negative. This finding implies that there should be another transient cellular event that can only be detected by EIM and occurs before calcium-flux-induced dynamic mass redistribution (i.e., ER micromotions) dominates the SPR and EIM signals.

A detailed subcellular analysis of one of the cells in group 2 (marked with an asterisk in Figure 4c) that displayed a remarkable transient positive EIM response is shown in Figure 5a. Transient positive EIM responses originated from EIM hot spots (R1 and R2 in Figure 5a, EIM image at +0.6 s), which then decayed to cold spots (R1 and R2 in Figure 5a, EIM image at +2.2 s) when the SPR signal began to rise (Figure 5e). The processes of Ca^{2+} release and refilling are enabled by various Ca^{2+} related ion channels, including IP_3 receptors, store-operated Ca^{2+} channels, and Ca^{2+} ATPase.[10a,12] The opening of these ion channels and the ionic transport through them increase the local conductivity of the ER/cell membrane, resulting in local transient EIM hot spots. For comparison, the cells were first treated with BAPTA-AM before histamine stimulation. BAPTA-AM can chelate intracellular calcium and inhibit further SPR/EIM responses (Figures 2c and 4b, gray circles), but it does not affect Ca^{2+} release from the ER induced by IP_3 elevation. In this case, the transient EIM hot spots should still be observable and even have a longer life time (Figure 5b, EIM images). As the consequent cellular events were inhibited by BAPTA-AM, the EIM signal did not decrease any more (Figure 5e, black dotted line). These results indicate that the EIM images can not only be used to temporally resolve the Ca^{2+} release events, but also provide information on the subcellular distribution of calcium-related ion channels and their activities during agonist-activated calcium flux (more examples are shown in Sections S6 and S7).

In summary, the calcium signaling at the early stage of GPCR stimulation was studied by a P-EIM technique that does not require any labels. Highly dynamic and transient responses were detected with single-cell and subcellular resolution. In-depth kinetic analyses of the single-cell SPR response quantitatively described the variations of the calcium flux activities in individual cells and revealed that a subpopulation of cells is more active towards agonist stimulation. The transient hot spots in the EIM images

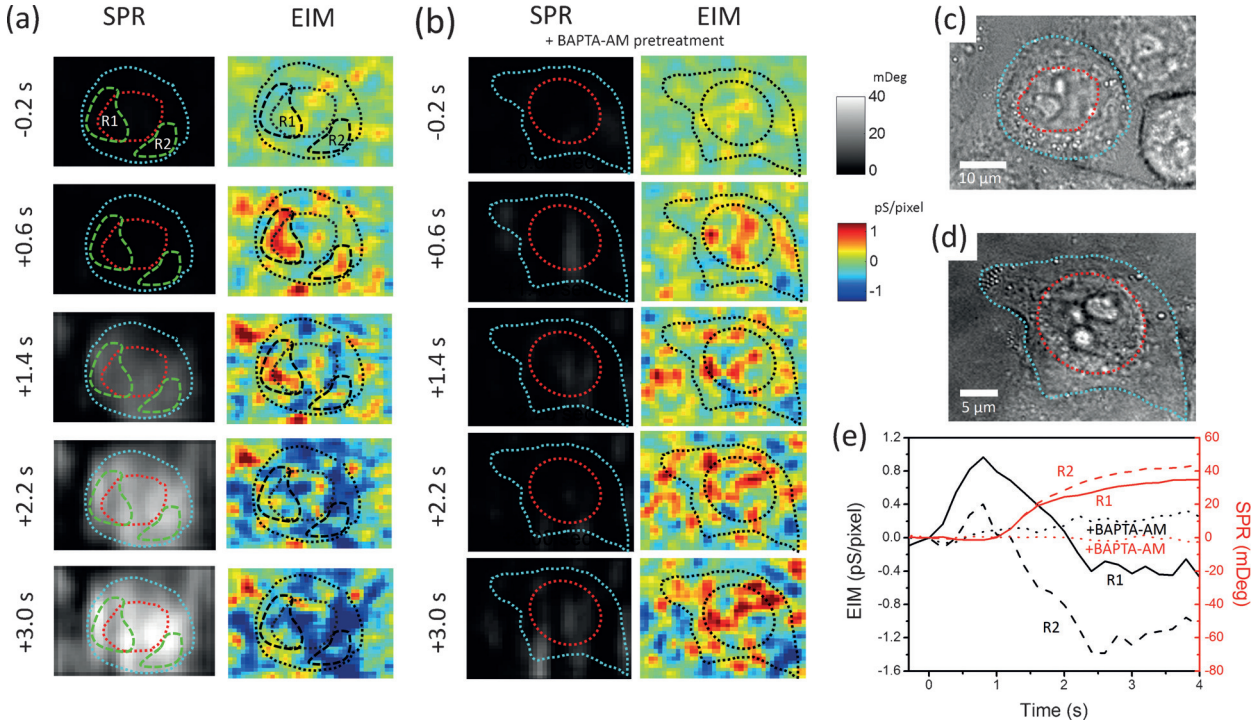

Figure 5. Differential SPR and EIM images of a single cell after stimulation with 18 μM histamine without (a) or with (b) pretreatment with 10 μM BAPTA-AM for 20 min. c, d) Bright-field images of the single cells studied in (a) and (b). The cyan and red dotted lines indicate the boundaries of the cells and the nuclei, respectively. e) EIM (black) and SPR (red) response curves of subcellular regions (R1 and R2 in (a)) stimulated by histamine, and of the single cell in (d) stimulated by histamine after 10 μM BAPTA-AM pretreatment. R1: solid lines; R2: dashed lines; single cell with BAPTA-AM pretreatment: dotted lines.

revealed the local distribution and activities of ion channels during agonist-activated calcium flux. Together, the SPR and EIM images characterized the heterogeneity of the behavior of single HeLa cells during a short period of GPCR activation. We believe that the P-EIM can be used to study other calcium-related cellular events in diverse time domains. We also expect that more second messenger molecules and cellular events will be studied by P-EIM, which should offer abundant information with high temporal and spatial resolution to better understand the complexity of the intrinsically stochastic behavior of single cells.

Acknowledgements

This work was financially supported by the National Natural Science Foundation of China (21235004 and 21327806).

Keywords: calcium · cell signaling · label-free methods · electrochemical impedance microscopy · surface plasmon resonance

How to cite: *Angew. Chem. Int. Ed.* **2015**, *54*, 13576–13580
Angew. Chem. **2015**, *127*, 13780–13784

[1] a) D. E. Clapham, *Cell* **2007**, *131*, 1047–1058; b) M. J. Berridge, *Nature* **1993**, *361*, 315–325.
[2] M. J. Berridge, P. Lipp, M. D. Bootman, *Nat. Rev. Mol. Cell Biol.* **2000**, *1*, 11–21.
[3] a) C. Wei, X. Wang, M. Chen, K. Ouyang, L. S. Song, H. Cheng, *Nature* **2009**, *457*, 901–905; b) J. W. Dani, A. Chernjavsky, S. J. Smith, *Neuron* **1992**, *8*, 429–440.
[4] a) A. Miyawaki, J. Llopis, R. Heim, J. M. McCaffery, J. A. Adams, M. Ikura, R. Y. Tsien, *Nature* **1997**, *388*, 882–887; b) M. Schäferling, *Angew. Chem. Int. Ed.* **2012**, *51*, 3532–3554; *Angew. Chem.* **2012**, *124*, 3590–3614.
[5] a) N. Yu, J. M. Atienza, J. Bernard, S. Blanc, J. Zhu, X. Wang, X. Xu, Y. A. Abassi, *Anal. Chem.* **2006**, *78*, 35–43; b) L. Wang, L. Wang, H. Yin, W. Xing, Z. Yu, M. Guo, J. Cheng, *Biosens. Bioelectron.* **2010**, *25*, 990–995; c) Y. Fang, A. M. Ferrie, N. H. Fontaine, J. Mauro, J. Balakrishnan, *Biophys. J.* **2006**, *91*, 1925–1940; d) R. Schröder, N. Janssen, J. Schmidt, A. Kebig, N. Merten, S. Hennen, A. Müller, S. Blättermann, M. Mohr-Andrä, S. Zahn, J. Wenzel, N. Smith, J. Gomeza, C. Drewke, G. Milligan, K. Mohr, E. Kostenis, *Nat. Biotechnol.* **2010**, *28*, 943–949; e) Q. J. Liu, C. S. Wu, H. Cai, N. Hu, J. Zhou, P. Wang, *Chem. Rev.* **2014**, *114*, 6423–6461.
[6] a) K. Hinterding, D. Alonso-Diaz, H. Waldmann, *Angew. Chem. Int. Ed.* **1998**, *37*, 688–749; *Angew. Chem.* **1998**, *110*, 716–780; b) L. S. De Clerck, C. H. Bridts, A. M. Mertens, M. M. Moens, W. J. Stevens, *J. Immunol. Methods* **1994**, *172*, 115–124.
[7] a) B. Huang, F. Yu, R. N. Zare, *Anal. Chem.* **2007**, *79*, 2979–2983; b) S. Wang, X. Shan, U. Patel, X. Huang, J. Lu, J. Li, N. Tao, *Proc. Natl. Acad. Sci. USA* **2010**, *107*, 16028–16032; c) J. Lu, W. Wang, S. Wang, X. Shan, J. Li, N. Tao, *Anal. Chem.* **2012**, *84*, 327–333; d) W. Wang, K. Foley, X. Shan, S. Wang, S. Eaton, V. J. Nagaraj, P. Wiktor, U. Patel, N. Tao, *Nat. Chem.* **2011**, *3*, 249–255.
[8] a) H. E. Hamm, *Proc. Natl. Acad. Sci. USA* **2001**, *98*, 4819–4821; b) K. L. Pierce, R. T. Premont, R. J. Lefkowitz, *Nat. Rev. Mol. Cell Biol.* **2002**, *3*, 639–650; c) P. Kolb, G. Klebe, *Angew. Chem.*

Int. Ed. **2011**, *50*, 11573 – 11575; *Angew. Chem.* **2011**, *123*, 11778 – 11780.

[9] a) B. C. Tilly, L. G. Tertoolen, A. C. Lambrechts, R. Remorie, S. W. de Laat, W. H. Moolenaar, *Biochem. J.* **1990**, *266*, 235 – 243; b) S. Muallem, T. M. Wilkie, *Cell Calcium* **1999**, *26*, 173 – 180; c) M. J. Lohse, V. O. Nikolaev, P. Hein, C. Hoffmann, J. P. Vilardaga, M. Bunemann, *Trends Pharmacol. Sci.* **2008**, *29*, 159 – 165.

[10] a) E. F. Corbett, M. Michalak, *Trends Biochem. Sci.* **2000**, *25*, 307 – 311; b) S. Carrasco, T. Meyer, *Annu. Rev. Biochem.* **2011**, *80*, 973 – 1000.

[11] M. Volpi, R. D. Berlin, *J. Cell Biol.* **1988**, *107*, 2533 – 2539.

[12] a) J. Meldolesi, T. Pozzan, *Trends Biochem. Sci.* **1998**, *23*, 10 – 14; b) J. P. Lièvremont, A. M. Hill, M. Hilly, J. P. Mauger, *Biochem. J.* **1994**, *300*, 419 – 427.

Received: June 30, 2015
Published online: September 4, 2015

